Structural assessment of liquid-crystalline side-chain poly(vinyl ether)s: dependence on terminal group, orientation and temperature

F. Sahlén, A. Hult and U. W. Gedde*
Department of Polymer Technology, Royal Institute of Technology, S-100 44 Stockholm, Sweden

and F. Ania and J. Martinez-Salazar
Instituto de Estructura de la Materia, Consejo Superior de Investigaciones Cientificas, Calle Serrano, 119-123, E-28006 Madrid, Spain
(Received 31 December 1993; revised 8 March 1994)

Oriented and non-oriented samples of two liquid-crystalline side-chain poly(vinyl ether)s, poly{4-[11-(vinyloxy)undecyloxy]-4-cyanophenylbenzoate} (poly(**1**)) and poly{4-[11-(vinyloxy)undecyloxy]-4-ethoxyphenylbenzoate} (poly(**2**)), have been studied by small-angle and wide-angle X-ray scattering techniques, polarized light microscopy and differential scanning calorimetry. The terminal group of the mesogenic unit played an important role in the organization of the side chains. With increasing temperature, poly(**1**) exhibited a smectic C, a transitional ordered smectic, a smectic A and finally an isotropic phase, whereas poly(**2**) showed a crystal B, a smectic A and an isotropic phase. Both polymers showed a glass transition at 310 K. The global alignment of the mesogenic groups did not affect the internal order of the smectic phases.

(Keywords: liquid-crystalline polymers; side-chain poly(vinyl ether)s; structural characterization)

INTRODUCTION

The microstructure of side-chain liquid-crystalline polymers has been studied in the past 15 years to clarify the influence of the molecular constituents – polymer backbone, mesogen, spacer group and terminal group – on the liquid-crystalline structures and phase transitions[1-3]. The mesogenic groups with a sizeable conjugated system linked to electron-donating and electron-accepting groups are hyperpolarizable, i.e. they have intrinsic non-linear optical properties[4]. The backbone chains give the material polymeric properties and the flexible spacer groups decouple the mesogenic units and allow them to form layer structures essentially unaffected by the motions of the backbone[5]. Side-chain liquid-crystalline polymers with hyperpolarizable mesogenic groups are potentially useful in electro-optics and photonics[6].

The physical structures of side-chain liquid-crystalline polymers have been assessed by polarized light microscopy, differential scanning calorimetry (d.s.c.), miscibility studies and X-ray diffraction, a subject that has been reviewed by Noël[7]. Based on hot-stage polarized light microscopy, the phase transition temperatures and the liquid-crystalline phases can be determined by texture characterization. D.s.c. provides information about the transition temperatures and the associated changes in enthalpy and entropy. Miscibility studies have primarily been used to determine the structural phases of low-molar-mass liquid crystals and in some cases of liquid-crystalline polymers[8]. X-ray diffraction provides the best means of determining the structural phases of liquid-crystalline side-chain polymers, although reliable structural assessment requires the preparation of aligned samples[9].

Cationic bulk polymerization of liquid-crystalline vinyl ether monomers at elevated temperatures yields relatively high-molar-mass polymers with a narrow molar-mass distribution[10]. Reactions are fast and give high yields. Polarized light microscopy and d.s.c. investigations of the liquid-crystalline polymers indicated the presence of crystalline phases at room temperature and enantiotropic smectic A mesophases at higher temperatures[10-12]. This paper presents further studies, using a combination of X-ray diffraction, polarized light microscopy and d.s.c., of the microstructure of liquid-crystalline side-chain poly(vinyl ether)s with phenylbenzoate as the mesogen, an undecanyl spacer, and cyano and ethoxy terminal groups. Samples of different orientations have been studied.

EXPERIMENTAL

Materials

p-Methoxybenzyltetramethylenesulfonium hexafluorophosphate was used as thermal initiator and phenacyltetramethylenesulfonium hexafluoroantimonate was used as photoinitiator. The syntheses of these compounds are described elsewhere[13].

Phenothiazine was obtained from Aldrich and used as

* To whom correspondence should be addressed

0032-3861/94/19/4041-07

photosensitizer for the photopolymerizations. All other reagents and solvents were obtained from Aldrich and Merck.

Synthesis of monomers

4-[11-(Vinyloxy)undecyloxy]-4-cyanophenylbenzoate (**1**) (*Figure 1*) was synthesized as reported elsewhere[10].

4-[11-(Vinyloxy)undecyloxy]-4-ethoxyphenylbenzoate (**2**) (*Figure 1*) was synthesized in the same way as **1** except that 4-ethoxyphenol was added instead of 4-cyanophenol in the final esterification reaction. The resulting solid was a white crystalline powder. Purity (h.p.l.c.) 99.9%. M.p. (d.s.c.) 339 K. ^{1}H n.m.r. ($CDCl_3$, tetramethylsilane (TMS)), δ (ppm): 1.25–1.50 (14 protons, $-(CH_2)_7-$, m), 1.35–1.55 (3 protons, CH_3CH_2O-, t), 1.60–1.73 (2 protons, $-CH_2CH_2-O-CH=CH_2$, p), 1.73–1.90 (2 protons, $-CH_2CH_2-OPh$, p), 3.62–3.72 (2 protons, $-CH_2-O-CH=CH_2$, t), 3.95 (1 proton, $CH_2=CHO-$ *trans*, d), 3.98–4.10 (4 protons, 2 from CH_3CH_2O-, 2 from $-CH_2CH_2-OPh$, m), 4.10–4.25 (1 proton, $CH_2=CHO-$ *cis*, d), 6.40–6.55 (1 proton, $CH_2=CHO-$, q), 6.90 (2 aromatic protons *ortho* from –O– of ethoxy group, d), 6.98 (2 aromatic protons *meta* from –C– of ester group, d), 7.10 (2 aromatic protons *meta* from –O– of ethoxy group, d), 8.12 (2 aromatic protons *ortho* from –C– of ester group, d). ^{1}H n.m.r. was performed in a Bruker 250 MHz apparatus.

Sample preparation and measurements

The initiator was added to the monomer as a dilute solution in CH_2Cl_2. The monomer–initiator blend was dissolved in CH_2Cl_2 and mixed while the solvent evaporated. The resulting solid mixture was then dried in a vacuum oven overnight. The monomer-to-initiator ratio was in all cases 250:1.

The polymerizations were carried out under isothermal conditions. Photoinitiated polymerization, i.e. illuminating the monomer-containing mixture kept between glass slides with an Osram Ultra-Vitalux lamp (300 W), was studied by polarized light microscopy (Leitz Ortholux POL BK II equipped with a Mettler hot-stage FP 82). Samples prepared for d.s.c. were thermally polymerized in aluminium pans in the d.s.c. apparatus (Perkin–Elmer DSC-7). The polymer samples prepared for the X-ray work were made by photopolymerization (Osram Ultra-Vitalux lamp, 300 W), between KBr pellets. The KBr pellets were dissolved in water to achieve free polymer films. Poly(**2**) was also polymerized by thermal initiation, on heating, in a glass capillary. This was possible due to the enantiotropic behaviour of monomer **2**.

Polymers with a high planar orientation were obtained by polymerizing the monomers in an oriented state. When polarized light microscopy was used, the planar alignment was induced by rubbed polyimide films, coated on the inside of the glass slides. Rubbed polyimide films coated on the inside of the KBr pellets created the orientation of the free polymer films used in the X-ray work. Monomers in the glass capillaries were oriented in a 0.3 T magnetic field inside the X-ray apparatus and the magnetic field was held constant throughout the X-ray diffraction experiment. Fibres of well defined diameters were inserted between the glass slides and between the KBr pellets to obtain polymer films with a uniform thickness of 30 μm.

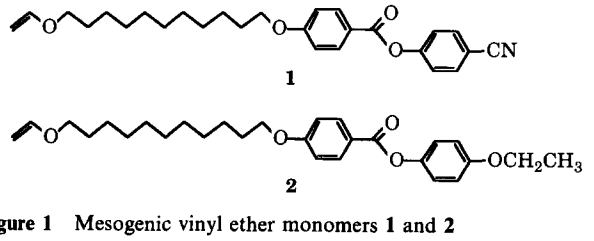

Figure 1 Mesogenic vinyl ether monomers **1** and **2**

Differential scanning calorimetry (Perkin–Elmer DSC-7, scanning rate 10 K min^{-1}) was used for thermal characterization. Polarized light microscopy (Leitz Ortholux POL BK II equipped with a Mettler hot-stage FP 82) was used for textural characterization at different temperatures. Small-angle X-ray scattering patterns were recorded (Statton camera using Ni-filtered Cu Kα radiation from a Philips PW 1830 generator and a Kiessig camera using fine focused Ni-filtered Cu Kα radiation from a Rigaku Denki generator equipped with a rotating anode). Heating of the samples was controlled by a resistive oven in the Statton camera and by the flow of a thermostatic bath in the Kiessig camera. Wide-angle X-ray scattering (Stadi/P instrument equipped with a curved position-sensitive detector, radius 220 mm, using monochromatic Cu $K\alpha_1$ radiation) was used for structural characterization.

The X-ray diffraction films obtained in the Statton camera were analysed in an image analysis system: Northern Light model B90 light table; Dage MTI 70 series camera; DTK 486–33 MHz PC; software Optimas by Bioscan Inc.; UN-Scorpion VGA-Framegrabber. The optical density distribution on the analysed films was transformed into data of scattered intensity as a function of the angle of diffraction (2θ).

RESULTS AND DISCUSSION

The cationic polymerizations of monomers **1** and **2** (*Figure 1*), initiated thermally or by a photochemical mechanism, were carried out under isothermal conditions in the bulk state. The use of sulfonium salt initiators in low concentrations yielded polymers of high purity with relatively high molar mass and a narrow molar-mass distribution. Photoinitiated polymerization produces polymers with a molar mass of about 20 000 g mol^{-1}, whereas thermally initiated polymerization results in polymers with a higher molar mass, a typical value being about 50 000 g mol^{-1} (refs. 10 and 12). The polydispersity ($\bar{M}_w/\bar{M}_n$) of the polymers was in both cases about 2.0. Orientation of the monomers by contact with a rubbed polyimide film caused a reduction in molar mass from the isotropic 20 000 g mol^{-1} to 13 000 g mol^{-1} (ref. 14). It is believed that impurities present in the rubbed polyimide film cause early termination of the polymerization[14].

Polarized light microscopy

Photopolymerization of monomers **1** and **2** in both the mesomorphic and isotropic states resulted in polymers showing enantiotropic behaviour.

Poly(**1**) displayed two mesomorphic phases as assessed by textural observation. On cooling the isotropic melt, a focal-conic fan texture typical of smectic A formed at 423 K. Further cooling resulted in a transition appearing at 305 K, which changed the focal-conic fan texture into

a paramorphotic sanded focal-conic fan texture. This phase shows a great similarity to the sanded texture found in low-molar-mass smectic C compounds[15] and in side-chain polyacrylates with terminal cyano groups[16]. The low-temperature phase was stable down to well below room temperature, and the sandiness disappeared on heating above the transition temperature at 349 K, at which a clear focal-conic fan texture reappeared.

Poly(**2**) exhibited two mesogenic phases as assessed by textural observation. On cooling the isotropic melt, a focal-conic fan texture very similar to that found in poly(**1**) and typical of the smectic A phase was formed at 396 K. Further cooling led to the formation of so-called transition bars appearing across the fans at 330 K (*Figure 2*). The bars gradually widened and met to form a focal-conic texture with smoother fans. The textural changes observed are similar to those appearing in low-molar-mass compounds exhibiting a low-temperature, paramorphotic smectic B phase[15]. The low-temperature phase was stable to temperatures well below room temperature. On heating poly(**2**) from low temperatures, the transition bars reappeared at 339 K, although they were more vague than before the thermal cycle. The focal-conic domains patterned with parabolic focal-conic defects, which are indicative of a smectic A phase, reappeared gradually on further heating.

Polarized light microscopy indicated that no change in the state of orientation of the aligned polymer samples accompanied the phase transitions. The sandiness of the low-temperature mesomorphic phase of poly(**1**) and the bars at the transition between the mesomorphic phases of poly(**2**) also appeared in the aligned samples.

X-ray scattering

X-ray scattering patterns of the high-temperature mesophase of aligned poly(**1**) showed diffuse equatorial wide-angle reflections corresponding to an intermesogenic distance of 0.44 nm (*Figure 3a*). Two sharp spots and at least two more orders of reflections were seen on the meridian at a small scattering angle corresponding to a layer thickness of 3.4 nm. The length of the extended mesogen was approximately 1.1 ± 0.1 nm. From infra-red spectroscopy data, the spacer group was known to show significant orientation with order parameter values in the range 0.3–0.4[17]. The fraction of bonds in the *trans* state (x_t) may be estimated by Boltzmann weighting:

$$x_t = \frac{1}{1 + 2\exp(-\Delta E/RT)}$$

(where ΔE, the energy difference between *trans* and *gauche* states, is set to 2500 J mol^{-1} (ref. 18)) to be 0.60 ± 0.10, and five to six of the spacer group bonds will be in any of the two *gauche* states. The end-to-end distance of the spacer group including the backbone chain is thus 1.2 ± 0.1 nm. This is an average value based on a simulation of 200 spacer group chains. The layer thickness including the mesogen and two spacer group layers is thus calculated to be 3.5 ± 0.3 nm, which is very close to the 3.4 nm observed. The high-temperature mesophase may thus be identified as an interdigitated smectic A_d phase (*Figure 4a*).

In a previous work based on polarized light microscopy and d.s.c. data, the low-temperature phase of poly(**1**) has been tentatively identified as a crystalline phase[11]. The X-ray scattering patterns of aligned poly(**1**) of the

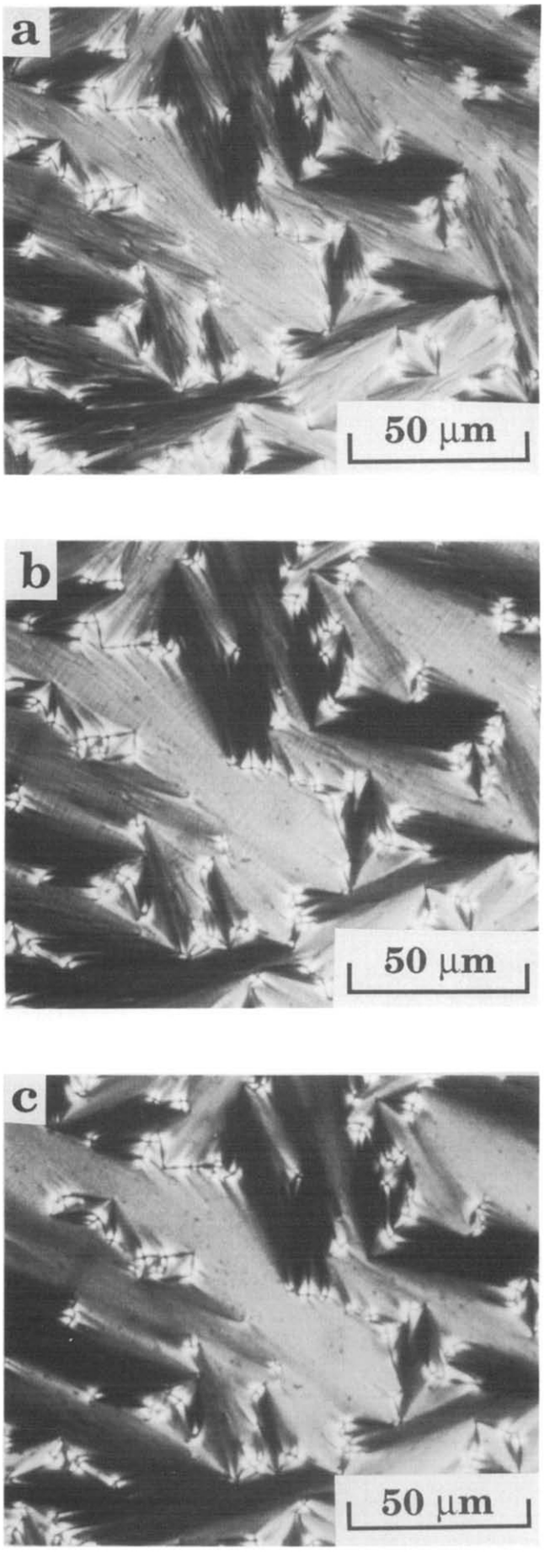

Figure 2 Polarized photomicrographs of non-oriented poly(**2**) taken on cooling at three different temperatures: (a) 385 K, focal-conic fan texture; (b) 330 K, development of transition bars crossing the fan structures; and (c) 295 K, focal-conic texture with smooth fans

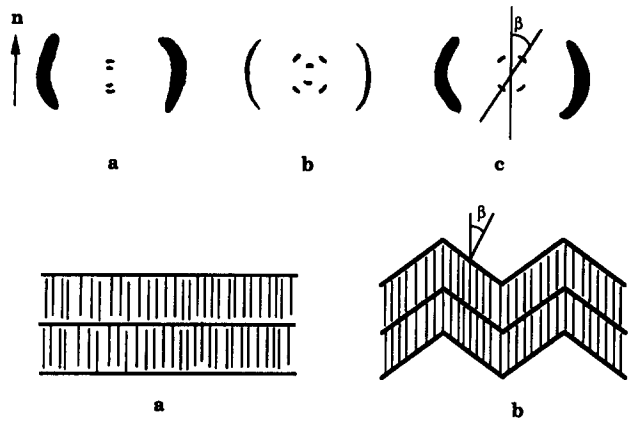

Figure 3 Diffraction patterns drawn from the X-ray films obtained from oriented poly(**1**): (a) at 363 K, smectic A phase; (b) at 353 K, transitional smectic phase; and (c) at room temperature, smectic C phase; here β is the tilt angle and n represents the director

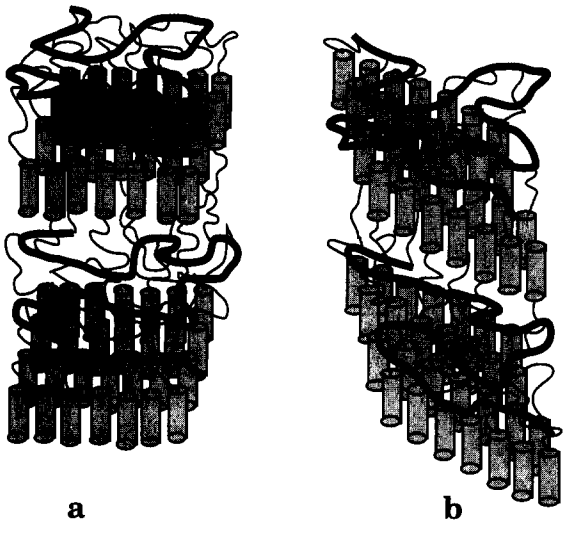

Figure 4 Schematic representation of (a) a smectic A_d phase and (b) a smectic C_d phase. The polymer backbones and the spacer groups form a disordered phase between the layers of ordered mesogenic groups

low-temperature phase consisted of a diffuse wide-angle equatorial reflection corresponding to an intermesogenic distance of 0.44 nm (*Figure 3c*). At small scattering angles, four sharp spots were located symmetrically displaced from the meridian (*Figure 3c*). This X-ray scattering pattern is typical of a smectic C structure[19]. The small-angle reflections represented a layer thickness of 3.1 nm and the tilt angle β was 25°, which, from the aforementioned arguments relating to the high-temperature phase, suggests a smectic C_d phase (*Figure 4b*). Aligned poly(**1**), cooled to liquid-nitrogen temperature and then reheated to room temperature, displayed the same X-ray diffraction pattern as that of the sample prior to this thermal treatment.

An unexpected mesophase (S_x) was observed on heating in the transitional temperature region between 338 and 353 K, i.e. between the temperature regions of the identified smectic phases (s_A and s_C). The X-ray scattering pattern of this new, intermediate phase is shown in *Figures 3b* and *5*. Most surprising is the sharpness of the wide-angle reflection in comparison with those obtained from the two 'surrounding' smectic A and C phases (*Figure 5*). The sharpness of the outer reflection at the equator, corresponding to an intermesogenic distance of 0.45 nm, indicates a more regular packing of the mesogens in the transitional phase than in the smectic A and C phases. The coexistence of the two sharp spots on the meridian and the four spots displaced from the meridian at low angles (*Figure 3b*) suggests a biphasic behaviour in the transitional temperature region.

The high-temperature mesophase of poly(**2**) (*Figures 6a* and *6b*) showed the same scattering pattern as the high-temperature mesophase of poly(**1**), i.e. a diffuse wide-angle reflection representing an average intermesogenic distance of 0.44 nm, and a single sharp small-angle reflection corresponding to a layer distance of 3.3 nm. With the same arguments as those presented for poly(**1**), this phase can be assigned as smectic A_d (*Figure 4a*).

The low-temperature mesophase showed a sharp, wide-angle reflection, 0.44 nm, and several orders of small-angle reflections, corresponding to a layer thickness of 3.3 nm (*Figures 6c* and *6d*). This pattern is similar to that of smectic B low-molar-mass compounds[20]. Two different forms of smectic B, crystal B and hexatic B, have been found[20]. Crystal B is characterized by long-range 'axial' positional order within the layers and also a regular layer thickness, whereas the hexatic B phase has only short-range 'axial', positional order within the layers[20]. In both cases the centre of gravity of the molecules in the smectic layers exhibits a hexagonal packing with long-range order[20]. The layers of the crystal B phase are regularly spaced and give rise to several orders of reflection. The low-temperature X-ray pattern of poly(**2**) showed at least four orders of small-angle reflection, suggesting the presence of a crystal B phase. Irradiation of poly(**2**) with the X-ray beam incident parallel to the mesogenic direction was carried out. The X-ray pattern resembled the pattern in *Figure 6c* but showed no inner, low-angle reflection. The circularity of the sharp wide-angle reflection, which was positioned at identical scattering angle as the one in *Figure 6c*, was probably due to the polydomain structure. *Figure 7* shows more

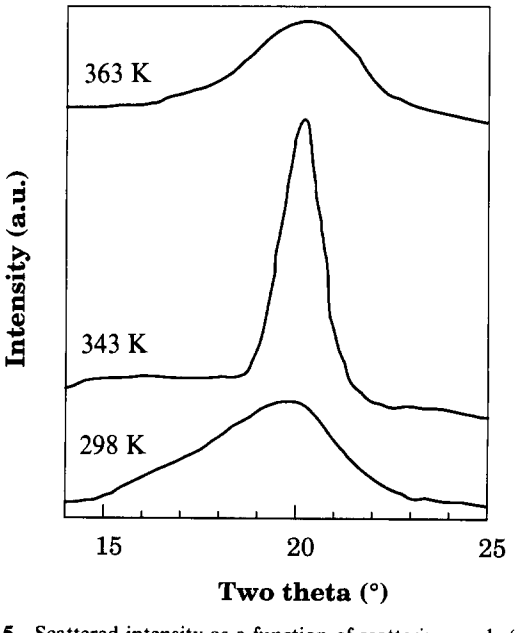

Figure 5 Scattered intensity as a function of scattering angle (2θ) for poly(**1**) taken at three different temperatures as shown in the graph

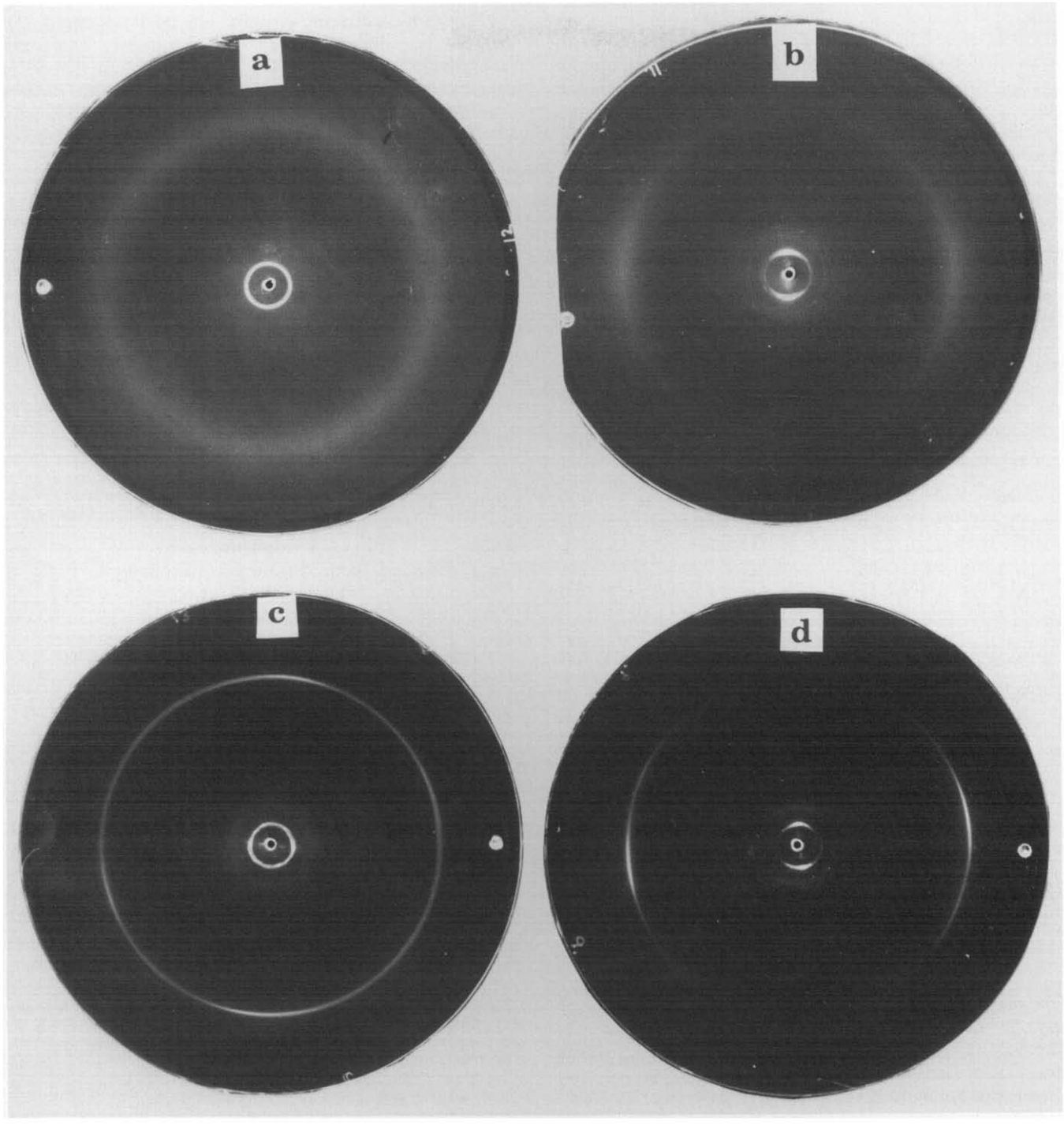

Figure 6 X-ray scattering patterns (Kiessig camera) of poly(**2**): (a) non-oriented smectic A phase at 385 K; (b) oriented smectic A phase at 385 K; (c) non-oriented crystal B phase at 295 K; and (d) oriented crystal B phase at 295 K. The sample-to-film distance was in all cases 97 mm

details from the equatorial wide-angle reflections and, in addition to the sharp peak centred at 20.6° (2θ), a broad scattering peak appears at the same 2θ value. The integrated intensities of the two overlapping peaks were almost identical. This indicated that the fraction of the ordered mesogenic groups that constitutes the crystal B phase in relation to the less ordered spacer and polymer backbone in poly(**2**) was about 0.50. The relative intensities of the two peaks remained unchanged in samples having different degrees of orientation.

The intensity–scattering angle profile integrated over the entire azimuthal angle space was the same for aligned and globally unoriented samples. The order within the smectic domains of poly(**1**) and poly(**2**) seems to be unaffected by the overall order parameter.

One of the important questions raised by the X-ray scattering results is why poly(**1**) is transformed into the tilted smectic C phase and poly(**2**) into an untilted crystal B phase. It is suggested that the terminal cyano group, which is a very strong dipole, plays a central role and that it forms a very strong bond with adjacent axially shifted mesogens (*Figure 8*). The axial shift is equal to 0.21 nm as calculated from the tilt angle (25°) and the intermesogen distance (0.44 nm). These strong interactions involve only pairs coming from main chains located in the same intermesogen group layer. The other non-

bonded interactions are weaker and some packing disorder evidently remains within the mesogen layers of poly(**1**). Poly(**2**), on the other hand, has no dipoles of similar strength and the packing of mesogens in the smectic A phase is improved, but there is no dominant, specific bond that forces the mesogens to displace axially and tilt.

Differential scanning calorimetry

The thermal transition data of **1**, **2**, poly(**1**) and poly(**2**) are presented in *Table 1* and *Figure 9*. A glass transition at 310 K was revealed for poly(**2**) (*Figure 9*). This is equivalent to the dielectric α relaxation found at the same temperature[21]. A glass transition was also found at 310 K for poly(**1**), but it was not as pronounced as that for poly(**2**). However, on cooling poly(**1**), the extensive first-order transition appearing at 305 K effectively hides the glass transition in this temperature range.

The small endothermic peak at 326 K appearing when poly(**1**) was heated was not associated with any change in the X-ray scattering pattern. The peak appeared at a temperature slightly above the glass transition and could tentatively be ascribed to the irreversible character of the glass transition. Samples of poly(**1**) were given various thermal treatments: (a) cooling from 350 to 230 K at a

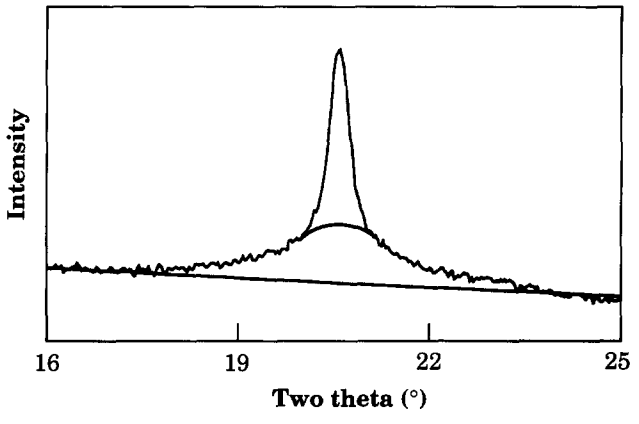

Figure 7 Wide-angle X-ray scattering pattern of poly(**2**) at room temperature recorded by a linear detector. The separation of ordered and disordered scattering components is shown in the figure

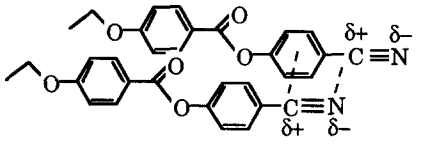

Figure 8 The dipole–dipole interaction between two adjacent mesogenic groups in poly(**1**) causing a tilt of the layers by 25°

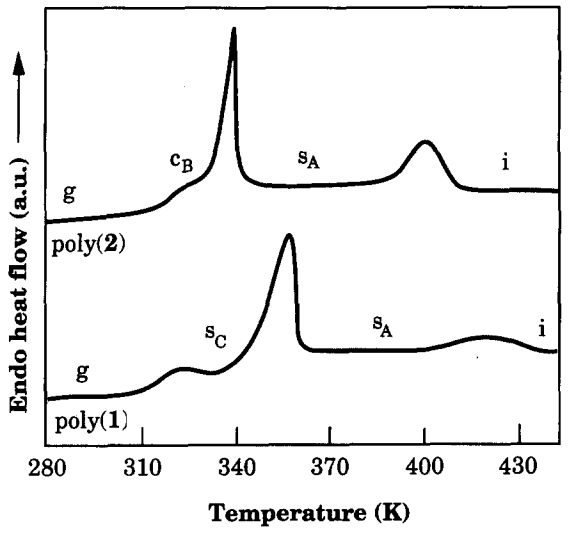

Figure 9 Heating thermograms of poly(**1**) and poly(**2**) (10 K min^{-1})

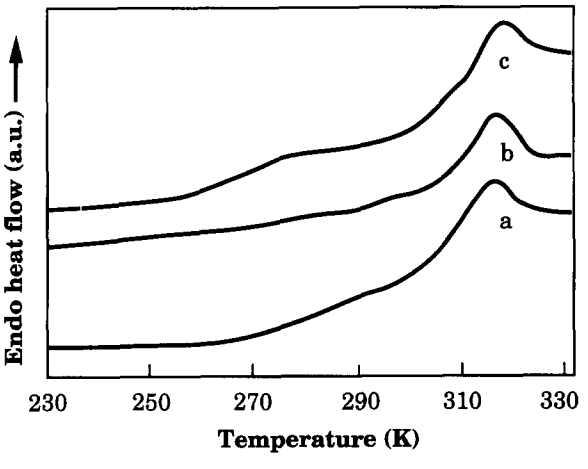

Figure 10 Heating thermograms obtained at different heating rates of poly(**1**) showing the endothermic peak at approximately 326 K: (a) cooling from 350 to 230 K at 1 K min^{-1} followed by heating at 10 K min^{-1}; (b) cooling from 350 to 230 K at 1 K min^{-1} followed by heating at 1 K min^{-1}; and (c) cooling from 350 to 230 K at 80 K min^{-1} followed by heating at 10 K min^{-1}

Table 1 Thermal transitions in the monomers and polymers studied[a]

Compound	Thermal transitions (K), enthalpy changes (kJ mol^{-1}) and entropy changes (J mol^{-1} K^{-1})[b]	
	Heating	Cooling
1	k341i	i337n323
2	k339n349i	i343n332s_A301k
Poly(**1**)	g310s_C326(0.9)s_C338s_X353(12.5)s_A427(2.0)i [2.9] [35.8] [4.68]	i423(1.4)s_A305(13.0)s_C308g [3.31] [42.6]
Poly(**2**)	g310c_B339(5.0)s_A407(5.0)i [14.7] [12.3]	i396(4.5)s_A330(4.7)c_B304g [11.4] [14.2]

[a]Data refer to second heating scan and first cooling scan according to d.s.c.

[b]Enthalpy and entropy changes per mole of repeat units; enthalpy changes are shown in parentheses and entropy changes in square brackets. The abbreviations used are as follows: g, glassy LC state; k, crystalline; c_B, crystal B; s_C, smectic C phases; s_A, smectic A; s_X, ordered, transitional smectic phase; n, nematic; i. isotropic melt

rate of 1 K min^{-1} followed by heating at two different rates, 10 and 1 K min^{-1}, and (b) cooling from 350 to 230 K at a rate of 80 K min^{-1} followed by heating at 10 K min^{-1}. In all cases the endothermic enthalpy associated with the '326 K peak' appeared to be the same (*Figure 10*), which is a finding in support of the hypothesis that this process is a true first-order transition. It should be pointed out that no corresponding exothermic first-order transition appeared on cooling poly(**1**), which is an argument in favour of the hypothesis that the low-temperature process is not a true first-order transition (*Figure 10*).

The 'novel' transitional phase in poly(**1**) was present at temperatures between 338 and 353 K, which matches the temperature region of the low-temperature first-order transition as recorded by d.s.c. (*Table 1*). The enthalpy change involved in the s_C–s_A process was considerably larger than that of the s_A–i process. The processes showed enantiotropic behaviour. Poly(**2**) displayed two first-order transitions appearing on both heating and cooling (*Table 1* and *Figure 9*). The enthalpy changes for the c_B–s_A and s_A–i transitions were similar, although the change was somewhat larger for the former process.

The total differences in entropy (Δs) and enthalpy (Δh) (per mole of repeat units) between the isotropic and room-temperature mesomorphic states were for poly(**1**) equal to 44 ± 2 J mol^{-1} K^{-1} and 14.9 ± 0.5 kJ mol^{-1} respectively and for poly(**2**) 26 ± 1 J mol^{-1} K^{-1} and 9.5 ± 0.5 kJ mol^{-1} respectively (*Table 1*). The total change in entropy was larger for poly(**1**) than for poly(**2**), which is surprising since X-ray scattering indicated that the low-temperature state of poly(**2**) is more ordered than that of poly(**1**). It is suggested that this apparently anomalous finding is due to the presence of specific non-bonded interactions between the strong cyano dipoles and phenylene groups appearing only in poly(**1**). It is further suggested that this interaction is the main cause for the tilted state of the low-temperature mesophase in poly(**1**). The strong specific interaction in poly(**1**) leads not only to a significant increase in Δh but also to some immobilization of the nearby groups. This is supported by dielectric relaxation studies[21] showing that the relaxation strength of the sub-glass process is lower in poly(**1**) than in poly(**2**).

CONCLUSIONS

Structural assessment of two liquid-crystalline side-chain poly(vinyl ether)s showed the influence of the terminal group on the organization of the mesogenic groups in the mesophases. A highly polar end-group such as the cyano group led to the formation of interdigitated smectic A and smectic C phases and, on heating, a more ordered smectic phase appeared at temperatures between the smectic A and C phases, whereas the less polar ethoxy terminal group led to interdigitated smectic A and crystal B phases. The vinyl ether polymers showed a glass transition at about 310 K.

ACKNOWLEDGEMENTS

Financial support from the National Swedish Board for Technical and Industrial Development (NUTEK) Grant 86-03476P, the Swedish Natural Science Research Council (NFR) Grant K-KU 1910-300, the Royal Institute of Technology (LUFT, School of Chemistry) and the Spanish CICYT Grant MAT90-0832 are gratefully acknowledged. We also thank Mr M. Trollsås for experimental assistance with ^{1}H n.m.r.

REFERENCES

1 Finkelmann, H. and Rehage, G. *Adv. Polym. Sci.* 1984, **60/61**, 99
2 Shibaev, V. P. and Platé, N. A. *Adv. Polym. Sci.* 1984, **60/61**, 173
3 McArdle, C. B. (Ed.) 'Side Chain Liquid Crystal Polymers', Chapman and Hall, New York, 1989
4 Burland, D. M., Miller, R. D., Reiser, O., Tweig, R. J. and Walsh, C. A. *J. Appl. Phys.* 1992, **71**, 410
5 Finkelmann, H., Happ, M., Portugall, M. and Ringsdorff, H. *Makromol Chem.* 1978, **179**, 2541
6 Prasad, P. N. and Reinhardt, B. A. *Chem. Mater.* 1990, **2**, 660
7 Noël, C. in 'Recent Advances in Liquid Crystalline Polymers' (Ed. L. L. Chapoy), Elsevier, London, 1985, Ch. 9
8 Noël, C. and Billard, J. *Mol. Cryst. Liq. Cryst. Lett.* 1978, **41**, 269
9 Azároff, L. V. *Mol. Cryst. Liq. Cryst.* 1987, **145**, 31
10 Jonsson, H., Sundell, P.-E., Gedde, U. W. and Hult, A. *Polym. Bull.* 1991, **25**, 649
11 Jonsson, H., Percec, V. and Hult, A. *Polym. Bull.* 1991, **25**, 115
12 Jonsson, H., Andersson, H., Sundell, P.-E., Gedde, U. W. and Hult, A. *Polym. Bull.* 1991, **25**, 641
13 Sundell, P.-E., Jönsson, S. and Hult, A. *J. Polym. Sci., Polym. Chem. Edn* 1991, **29**, 1535
14 Andersson, H., Gedde, U. W. and Hult, A. *Polymer* 1992, **33**, 4014
15 Gray, G. W. and Goodby, J. W. 'Smectic Liquid Crystals – Textures and Structures', Leonard Hill, London, 1984
16 Kostromin, S. G., Sinitzyn, V. V., Talrose, R. V., Shibaev, V. P. and Platé, N. A. *Makromol. Chem., Rapid Commun.* 1982, **3**, 809
17 Andersson, H., Gedde, U. W. and Hult, A. *Mol. Cryst. Liq. Cryst.* in press
18 Flory, P. J. 'Statistical Mechanics of Chain Molecules', Hanser, Munich, 1989
19 Luckhurst, G. R. and Gray, G. W. in 'The Molecular Physics of Liquids', Academic Press, New York, 1979, Ch. 13
20 Albertini, G., Fanelli, E., Melone, S., Rustichelli, F. and Torquati, G. *Solid State Commun.* 1984, **49**, 1143
21 Gedde, U. W., Liu, F., Hult, A., Sahlén, F. and Boyd, R. H. *Polymer* 1994, **35**, 2056